EVALUATING THE ADEQUACY OF A MATHEMATICAL MODEL OF THE PIERCING OF A BILLET INTO AN ULTRA-THICK-WALLED SHELL ON A TWO-HIGH ROTARY ROLLING MILL

V. P. Romanenko and D. V. Sizov   UDC 621.774.353

A physical experiment involving the piercing of a billet into an ultra-thick-walled shell is carried out on two-high mill 130D at the Moscow State Institute of Steel and Alloys. With the same process parameters as in the experiment, a mathematical model of the piercing operation is constructed by using the finite-element computing system in the software Deform 3D. The degree of agreement between the mathematical model and the physical experiment is evaluated on the basis of such indices as the geometric parameters of the pierced shell, the helix angle, and one of the kinematic characteristics – the time that elapses from the moment the billet contacts the rolls to the moment it contacts the mandrel.

***Keywords:** finite-element method, two-high rotary rolling mill, piercing, wall-thickness, pitch of a helix, assessment of adequacy, parameter comparison, Student's t-criterion.*

One of the most promising methods of studying metal-shaping operations is mathematical modeling by the finite-element method [1] in special computer programs. The modeling is based on the theoretical behavior of media under different loading conditions, especially within the framework of the theory of plasticity [2]. Positive results have already been obtained from the computer modeling of certain processes in extrusion, forging, stamping, rotary rolling, and other types of metal-shaping operations [3].

The Moscow Institute of Steel and Alloys (MISiS) is conducting a study of the process of piercing semifinished products into ultra-thick-walled shells on a rotary rolling mill. One of the methods being used in this research is mathematical modeling by the finite-element method in the software Deform 3D. The most important issue in regard to the expediency of using mathematical modeling to study piercing is the ability of the mathematical model to adequately describe the characteristics of the actual piercing operation.

In this article, we present results from a study of the adequacy of a mathematical model developed to describe the piercing of a semifinished product into an ultra-thick-walled shell on a two-high rotary rolling mill. The adequacy of the model was evaluated based on such indices as the geometric parameters of the pierced shell, the helix angle, and one of the kinematic characteristics – the time that elapses between the moment the semifinished product comes into contact with the rolls and the moment it comes into contact with the mandrel. The base dimensions of the tube are the dimensions imparted to it in a physical experiment.

Physical experiment. To study the change in the shape of the metal during its deformation in a two-high rotary rolling mill, we used a circular billet with a diameter of 100 mm and a length of 300 mm as the initial specimen. The billet was made from wheel steel of grade T in accordance with the State Standard GOST 10791-2011. The billet was pierced on prototype two-high rotary rolling mill 130D at MISiS (Fig. 1).
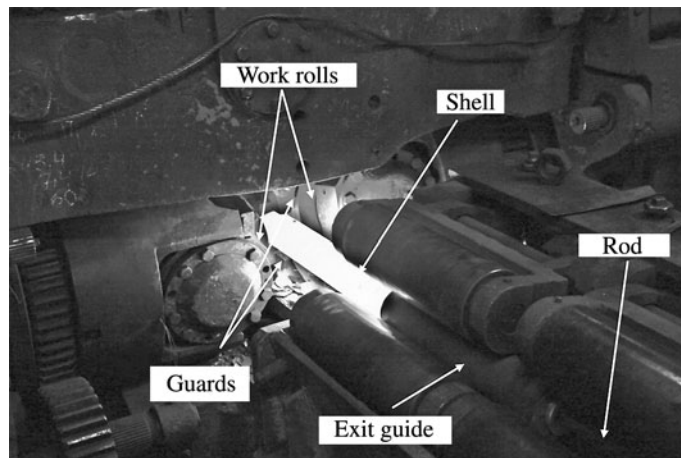

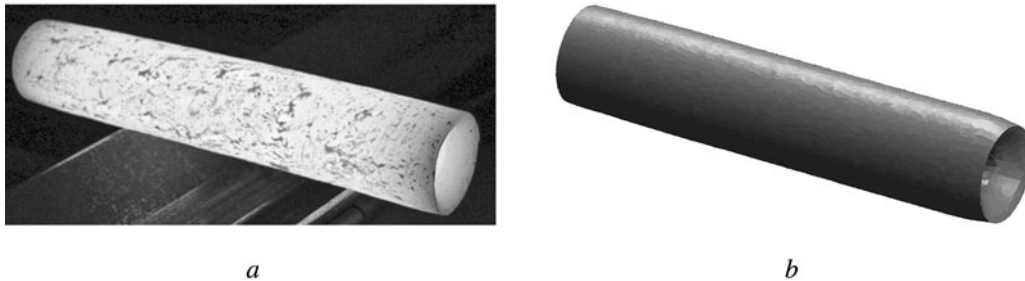Fig. 1. Deformation zone of piercing mill 130D at MISiS.

Fig. 2. Ultra-thick-walled shell obtained by piercing in a two-high rotary rolling mill: *a*) physical experiment; *b*) mathematical modeling.

The working element of the piercing mill was designed by the method presented in [4]. The working element used for piercing consisted of the following: biconical rolls with a diameter of 435 mm at the gorge, a length of 360 mm, inlet-cone angle $\phi_1 = 2.5°$, and outlet-cone angle $\phi_2 = 3°$; a 29-mm-diam. mandrel; guards, a mandrel rod, and entry and exit guides.

The billet was heated to 1200°C in a reverberatory furnace with selenite heaters. Holding time inside the furnace was 100 min, which was sufficient to ensure that the billet was uniformly heated over its entire volume. This alleviated the effect of one of the factors that is most responsible for fluctuations in the wall-thickness of semifinished products – nonuniform heating of the initial semifinished product.

The piercing was done with the following process parameters: reduction in the gorge $\varepsilon = 15\%$; feed angle $\beta = 12°$; ovalization factor $\xi = 1.1$ mm/mm; reduction in front of the nose of the mandrel $\varepsilon_{m.n.} = 12\%$; roll speed 60 rpm.

The reduction ahead of the mandrel nose was determined in such a way as to ensure that the maximum tensile forces were on the roll side and that the reduction was within the 3–12% range recommended in [5] for the cross section in which the billet is gripped the second time.

The geometric parameters of the pierced shell (Fig. 2*a*) were evaluated based on its outside diameter and the thickness of its wall. The measurements were made by the method described in [6]. Measurements of the thickness of the shell's wall were made at eight points over a distance of 100 mm. The measurements were made in two mutually perpendicular directions along the shell at points 40 mm apart, including both ends and the middle (Fig. 3).

The diameter and wall-thickness measurements were analyzed by the method presented in [7]. The analysis involved calculating the outside diameter of the shell $\overline{D}$, the standard deviation of outside diameter s_D, the variance of diameter σ_D^2, the average wall-thickness $\overline{S}$, the standard deviation of wall-thickness s_S, and the variance of wall-thickness σ_S^2. The results
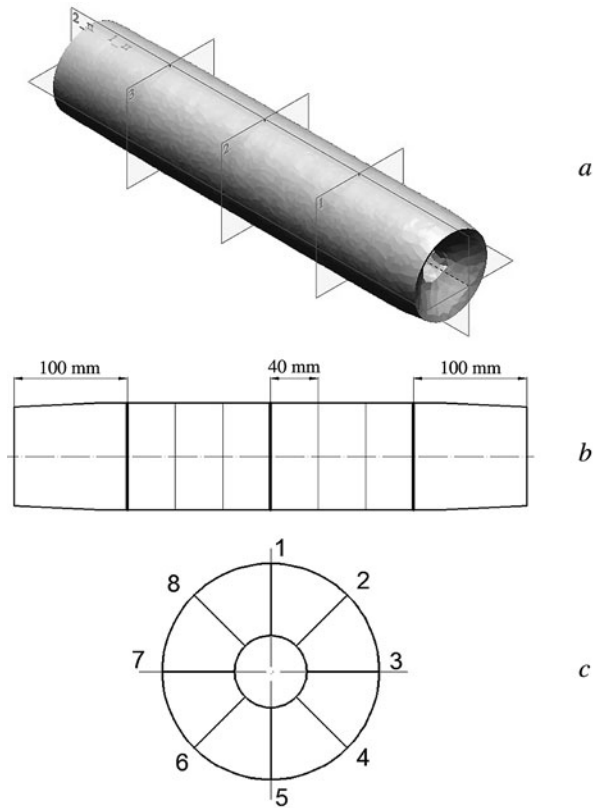
Fig. 3. Method of measurement of the geometric parameters: *a*) secant planes for measuring geometric parameters; *b*) cross section for measuring values of diameter and wall-thickness; *c*) eight points for measuring wall thickness over a cross section.
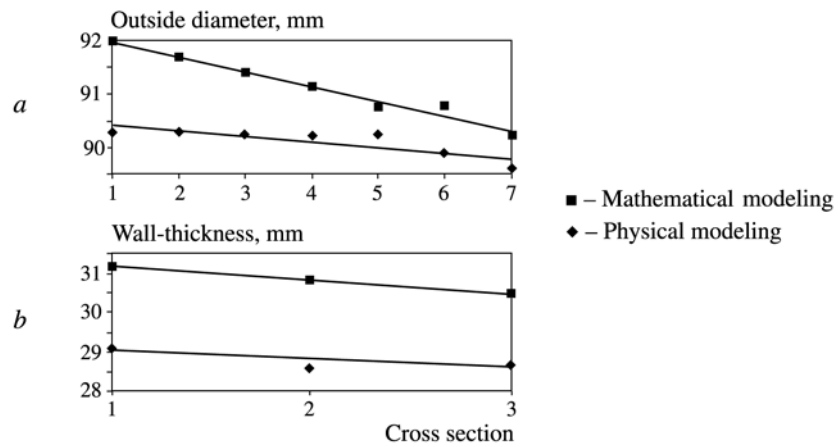

Fig. 4. Distribution of the average diameters (*a*) and average wall-thicknesses (*b*) by shell cross section from the front end to the back end (linear approximation).

of the measurements and calculations of the outside diameter of the shell used for the physical experiment are shown in Table 1, and the corresponding results for wall-thickness are shown in Table 2.

Analysis of the outside diameter of the pierced shell yielded the mean value $\bar{D} = 90.1$ mm. The calculations showed that the standard deviation is within ±0.29 mm or ±0.32% of the shell's average diameter.

TABLE 1. Analysis of Measurements of the Shell's Outside Diameter Obtained by Physical/Mathematical Modeling

No. of measurement	Diameter D_i, mm		Average diameter of cross section $D_{av(i)}$, mm	Deviation of the diameters from the mean value ΔD_i, mm		Square of the difference in the diameters ΔD_i^2	
	1	2		1	2	1	2
1	90.5/91.94	90.1/92.02	90.3/91.98	0.386/0.814	–0.014/0.894	0.149/0.663	$2 \cdot 10^{-4}$/0.800
2	90.2/91.69	90.4/91.67	90.3/91.68	0.086/0.564	0.286/0.544	$7.3 \cdot 10^{-3}$/0.318	0.082/0.296
3	90.4/91.17	90.1/91.61	90.25/91.39	0.286/0.044	–0.014/0.484	0.082/0.002	$2 \cdot 10^{-4}$/0.235
4	90.1/91.28	90.3/90.94	90.2/91.11	–0.014/0.154	0.186/–0.186	$2 \cdot 10^{-4}$/0.024	0.034/0.034
5	90.1/90.59	90.4/90.84	90.25/90.72	–0.014/–0.536	0.286/–0.286	$2 \cdot 10^{-4}$/0.287	0.082/0.082
6	90/90.78	89.8/90.80	89.9/90.79	–0.114/–0.346	–0.314/–0.326	0.013/0.120	0.099/0.106
7	89.5/90.29	89.7/90.14	89.6/90.22	–0.614/–0.836	–0.414/–0.986	0.377/0.698	0.172/0.972
Average diameter of shell $\overline{D}$, mm				90.1/91.13			
Variance σ_D^2, mm^2				0.084/0.36			
Standard deviation s_D, mm				0.291/0.6			
Average accuracy of shell diameter u_D, %				0.32/0.66			

TABLE 2. Analysis of Measurements of the Shell's Wall-Thickness Obtained by Physical/Mathematical Modeling

No. of measurement	Wall-thickness S_{ij}, mm			Deviation of wall-thickness from the mean value ΔS_{ij}, mm			Square of the difference in wall-thickness ΔS_{ij}^2, mm		
	entry side	middle	exit side	entry side	middle	exit side	entry side	middle	exit side
1	28.8/31.3	28.7/30.8	29.5/30.3	$5.8 \cdot 10^{-3}$/0.481	–0.074/–0.029	0.706/–0.539	$3.4 \cdot 10^{-5}$/0.231	$5.5 \cdot 10^{-3}$/$8.51 \cdot 10^{-4}$	0.498/0.291
2	29.0/31.0	28.2/30.4	28.3/30.55	0.206/0.131	–0.634/–0.419	–0.494/–0.389	0.042/0.017	0.402/0.176	0.244/0.151
3	29.0/31.3	28.2/30.9	28.8/30.6	0.206/0.491	–0.634/0.081	$5.8 \cdot 10^{-3}$/–0.259	0.042/0.241	0.402/$6.53 \cdot 10^{-3}$	$3.4 \cdot 10^{-5}$/0.067
4	29.4/31.2	28.0/31.1	28.7/30.5	0.606/0.361	–0.754/0.241	–0.094/–0.359	0.367/0.130	0.569/0.058	$8.87 \cdot 10^{-3}$/0.129
5	29.2/31.2	28.3/30.7	28.4/30.6	0.406/0.311	–0.514/–0.169	–0.394/–0.239	0.165/0.097	0.264/0.029	0.155/0.057
6	29.3/31.0	28.8/30.9	28.6/30.6	0.506/0.181	$5.8 \cdot 10^{-3}$/0.071	–0.194/–0.239	0.256/0.033	$3.4 \cdot 10^{-5}$/$5.02 \cdot 10^{-3}$	0.038/0.057
7	29.1/31.2	29.2/31.0	28.7/30.5	0.306/0.311	0.406/0.121	–0.094/–0.369	0.094/0.097	0.165/0.015	$8.9 \cdot 10^{-3}$/0.136
8	29.0/31.3	29.3/30.9	28.6/30.6	0.206/0.441	0.506/0.071	–0.194/–0.279	0.042/0.194	0.256/$5.02 \cdot 10^{-3}$	0.038/0.078
S_{jav}	30.10/31.18	29.58/30.84	29.70/30.51						
Average thickness of the shell wall $\overline{S}$, mm				28.8/30.84					
Variance σ_S^2, mm^2				0.18/0.10					
Standard deviation s_S, mm				0.42/0.32					
Average accuracy of wall-thickness u_S, %				1.46/1.03					

Study of the character of the diameter distribution along the shell revealed that its average value in each of the cross sections that were examined decreased linearly from the beginning to the end of the shell. The difference in diameter between the two outermost cross sections was 0.7 mm (Fig. 4*a*).

TABLE 3. Analysis of Measurements of the Helix Angle; Physical/Mathematical Modeling

| No. of measurement	Helix angle ψ_i, deg.	Deviation of the helix angle from the mean value $\Delta\psi_i$	Square of the difference in the helix angles $\Delta\psi_{ij}^2$
1	12.4/11.23	–0.17/0.41	0.03/0.17
2	11.8/11.16	0.43/0.48	0.19/0.23
3	12.7/12.17	–0.47/–0.53	0.22/0.28
4	12.4/11.83	–0.17/–0.19	0.03/0.04
5	11.9/11.53	0.33/0.11	0.11/0.01
6	12.2/11.9	0.03/–0.26	$1.1 \cdot 10^{-3}$/0.07
Average value of the helix angle $\bar{\psi}$, deg.			12.2/11.6
Variance σ_ψ^2			0.11/0.16
Standard deviation s_ψ, deg.			0.34/0.40
Average accuracy of the helix angle u_ψ, %			0.94/1.37
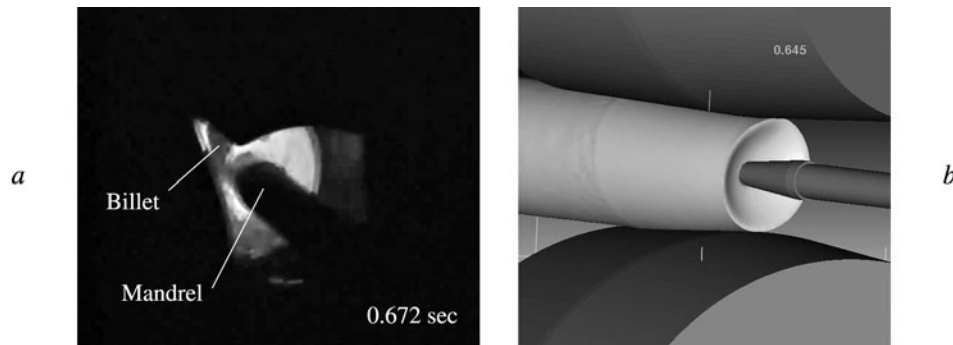
Fig. 5. Moment of contact between the billet and the mandrel: *a*) physical modeling; *b*) mathematical modeling (the guides are hidden).

The average thickness of the wall of the pierced shell was 28.8 mm. The standard deviation was ±0.42 mm or ±1.46% of the average wall-thickness. The difference between the average values of wall-thickness in the two outermost cross sections was 0.4 mm (Fig. 4*b*). The elongation factor for the shell $\propto$ = 1.42.

The helix angle was measured using marks made on the surface of the shell, and its average value, variance, and standard deviation were determined (Table 3). The average value of the helix angle in the physical experiment was 12.2° and the standard deviation was equal to ±0.34°.

One of the kinematic parameters that characterize the piercing operation is the time that elapses between the moment when the billet comes into contact with the rolls and the moment it comes into contact with the mandrel. This parameter was studied by obtaining video images of the piercing operation, analyzing them frame by frame, and determining when these two moments occurred. The video was recorded at a frame rate of 25 sec^{-1} and the accuracy of the measurement was ±0.02 sec. The experiment showed that 0.672 sec transpired between the moment the billet contacted the rolls and the moment it contacted the mandrel (Fig. 5).

Mathematical modeling. We chose the finite-element-based computing system Deform 3D to mathematically model the rotary piercing of a billet to convert it into an ultra-thick-walled shell. The system makes it possible to solve three-dimensional problems involving the plastic flow of metal, elastic deformation, heat exchange, and other matters connected with the

study of metal-shaping operations [8]. The geometric parameters of the rolls in the deformation zone corresponded to the geometric parameters of the working element of the 130D piercing mill.

Such parameters of the piercing operation as the reduction in the gorge, feed angle, ovalization factor, the reduction in front of the nose of the mandrel, and roll speed were the same in mathematical modeling as in the physical experiment.

The following assumptions were made in the finite-element modeling of rotary piercing:

1) the working element was regarded as a consisting of perfectly rigid bodies with a constant temperature;

2) friction between the billet and the working element conformed to the Amontons–Coulomb dry-friction law and the friction coefficient was constant over the entire surface of contact;

3) the piercing process was isothermal throughout the piercing operation; and

4) thermal expansion of the metal during heating and its thermal contraction during cooling were negligible.

The properties chosen as the rheological characteristics of the billet material were the rheological properties of steel AISI 1060, which has a carbon content that is close to the carbon content of wheel steel of grade T made in accordance with GOST 10791–2011.

After modeling of the plastic deformation of the metal, the geometric model of the pierced shell was cut in two mutually perpendicular longitudinal planes and three cross sections. The contours of the three-dimensional model in the two-dimensional plane were then exported into AutoCAD, where the diameters and wall-thicknesses were measured in accordance with the method used in the physical experiment (see Fig. 3).

Table 1 shows the results of measurement and calculation of the outside diameter of the three-dimensional model of the pierced shell, and Table 2 shows the corresponding results for wall-thickness.

The average diameter of the shell was 91.13 mm and the standard deviation was within ±0.6 mm, or ±0.66% of the average diameter of the shell. The average thickness of the shell wall was 30.84 mm. The standard deviation of wall-thickness was within ±0.32 mm, or ±1.03% of the average wall-thickness. The elongation factor in the mathematical model was $\propto = 1.35$ for the assigned process parameters.

When we examined the changes in the average diameter in different cross sections along the shell and the average wall-thickness for the cross sections, we found that the values tended to decrease from the front end of the shell to its back end. Here, the difference between the average diameters in the two outermost cross sections was 1.8 mm (see Fig. 4a), while the difference between the average values of wall-thickness was 0.7 mm (see Fig. 4b).

The average value of the helix angle in the mathematical modeling was 11.6° and the standard deviation was ±0.40° (see Table 3).

The time that elapsed between the moment the billet contacted the rolls to the moment it contacted the mandrel was 0.645 sec (Fig. 5). Here, the time step in the computation was 0.0015 sec and measurement accuracy was ±0.0075 sec.

An evaluation *of the adequacy of the mathematical model* constructed to describe the piercing of a solid billet into an ultra-thick-walled shell on a two-high rotary rolling mill was performed using such parameters as the convergence of the geometric parameters, the helix angles, and the times from the moment of contact with the rolls to the moment of contact with the mandrel.

The geometric parameters were compared based on the outside diameter, wall-thickness, and elongation factor. Comparison of the outside diameters showed that their average value was 1.0 mm, or 1.1% of the average diameter of the shell in the physical experiment. The large value of outside diameter pertains to the geometry of the pierced obtained by mathematical modeling. Comparison of the character of distribution of the outside diameters along the shell showed that in both cases the average diameter in each cross section decreased from the shell's front end to its back end (see Fig. 4a).

The difference in the wall-thickness of the shell in the physical and mathematical modeling operations was roughly 2.0 mm, or 7% of the average wall-thickness in the physical experiment. The average wall-thickness in each cross section decreased from the front to the back of the shell in both cases (Fig. 4b). The elongation factor in the physical experiment, $\propto = 1.42$, was 0.07 greater than the elongation factor in the mathematical modeling ($\propto = 1.35$).

In examining the files of data from measurements of outside diameter, it is necessary to check for equality of the average values in two data samples for the physical experiment and the mathematical modeling. Student's *t*-criterion was used for this purpose [9].

Student's *t*-criterion was found to have a value of 5.7 when two samples of data on *outside diameter* were examined with the number of degrees of freedom $n = 26$, which is equal to the sum of the number of measurements for the physical and mathematical modeling minus two. The tabulated value of Student's criterion for the chosen minimum confidence level $p = 0.001$ is equal to 3.7. The value of Student's *t*-criterion that was found for two groups of data samples for outside diameter was greater that the tabulated value for the same probability, which shows that these two samples do not belong to the same population of values.

With the number of degrees of freedom $n = 46$, Student's *t*-criterion had a value of 19.05 for two data samples for *wall-thickness*. The tabulated value of the *t*-criterion for a confidence level $p = 0.001$ is equal to 3.51. Given the same probability, the value of the *t*-criterion obtained here for the two wall-thickness data samples is significantly greater than the tabulated value. This means that these two samples do not belong to the same population.

The helix angle was 12.2° in the physical modeling and 11.6° in the mathematical modeling. With similar values for the standard deviation (±0.34 and ±0.40), the difference between the mean values of the helix angle was 0.6°. The lower value was obtained from the mathematical modeling.

The time of passage of the billet from the point of contact with the rolls to the point of contact with the mandrel was 0.672 sec for the physical experiment and 0.645 sec for the mathematical modeling. Here, the ranges of the measurement errors intersect (±0.02 sec for the experiment and ±0.0075 sec for the modeling), which means that this parameter is identical for both of the cases that were examined.

Conclusions. The adequacy of a finite-element model of the rotary piercing of billets into ultra-thick-walled shells on a two-high rotary rolling mill was studied in comparison to a physical experiment conducted with the same process parameters. A high degree of agreement was obtained between the two sets of results with respect to such geometric parameters as outside diameter, wall-thickness, the helix angle and one of the kinematic parameters – the time that elapses from the moment the billet comes into contact with the rolls to the moment it comes into contact with the mandrel. The difference between the data obtained by mathematical modeling and physical experimentation was minimal: the differences were 1.1% for outside diameter, 7% for wall-thickness, and 0.027 sec for the travel time of the billet between the rolls and the mandrel.

The results obtained in this investigation can be used as a foundation for further study of the piercing of ultra-thick-walled shells in a two-high rotary rolling mill by finite-element modeling, the goals here being to improve the production process, optimize the parameters of the piercing mill's working element, and improve the quality of products obtained from such shells. Shells of this type are also presently being used by scientists at the Moscow Institute of Steel and Alloys as semifinished products in research aimed at developing a new technology for making axisymmetric finished products with superior mechanical and service properties.

REFERENCES

1. G. Ya. Gun, *Mathematical Modeling of Metal-Shaping Operations* [in Russian], Metallurgiya, Moscow (1983).
2. A. A. Il'yushin, *Plasticity* [in Russian], Logos, Moscow (2004).
3. Y. Chastel, A. Diop, S. Fanini, et al., "Finite element modeling of tube piercing and creation of a crack," *Int. J. Material Forming*, **1**, 355–358 (2008).
4. B. A. Romantsev, A. V. Goncharuk, N. M. Vavilkin, and S. V. Samusev, *Metal-Shaping* [in Russian], MISiS, Moscow (2008).
5. I. N. Potapov, A. P. Kolikov, V. N. Danchenko, et al., *Technology of Tube Production: Text for Higher Educational Institutions* [in Russian], Metallurgiya, Moscow (1994).
6. V. P. Romanenko, D. V. Sizov, and G. P. Illarionov, "Experimental studies of the geometric parameters of the piercing of ultra-thick-walled shells," *Izv. Vyssh. Uchebn. Zaved., Chern. Metall.*, No. 12, 31–34 (2012).
7. M. F. Stoletnii and E. D. Klempert, *Accuracy of Tubes* [in Russian], Metallurgiya, Moscow (1975).
8. V. P. Romanenko and D. V. Sizov, "Modeling the rotary piercing of large-diameter semifinished products in a two-high mill by the finite element method," *Izv. Vyssh. Uchebn. Zaved., Chern. Metall.*, No. 3, 12–16 (2011).
9. H. Schenck, *Theories of Engineering Experimentation*, Taylor and Francis, Oxford (1979).